Desalination and Water Treatment
www.deswater.com

doi: 10.5004/dwt.2019.23893

161 (2019) 48–55
September

Once-through multistage flash desalination installation combined with thermal vapour compression MSF-OT/TVC

Ahlem Sellami*, Mongi Ben Ali, Mouna Lakhdar, Lakdar Kairouani

Université de Tunis El Manar, Ecole Nationale d'Ingénieurs de Tunis, Unité de Recherche Energétique et Environnement, Tunis Belvédère, BP 37, 1002, Tunisie, Tel. +216 24 574 044; email: ahlem.sellami@yahoo.fr (A. Sellami)

Received 28 April 2018; Accepted 29 January 2019

ABSTRACT

Novel configurations for the once-through multistage flash desalination MSF-OT process are proposed to improve its performance indicators. In these configurations, steam jet ejectors are used to compress vapour entrained from stages of the installation, which is then used to produce heating steam for the heat input section. Three configurations of once-through multistage flash desalination installation combined with thermal vapour compression (MSF-OT/TCV) are investigated, which includes vapour entrainment and compression from different stages. The TVC unit uses one or two jet steam ejectors in series, in order not to exceed the limit value of the compression ratio. The study includes the development of mathematical models for the three configurations, followed by the description of the method used to solve the equation systems obtained. This method uses the solver fsolve of MATLAB software. The analysis of the configurations is based on comparison of the thermal performance ratio, and the specific feed seawater flow rate, as a function of the top brine temperature and location of vapour entrainment. The results obtained indicate that entrainment vapour and compression by the steam jet ejector from high temperature stages give higher thermal performance ratio, than for vapour entrainment from low temperature stages. Results show that the increase in thermal performance ratio of the best MSF-OT/TCV configuration over the conventional MSF-OT configuration varies between 42% and 57%. However, this improvement is accompanied by a slight degradation in the specific feed seawater flow rate, whose value varies from 0.26% to 2.1%.

Keywords: Once-through multistage flashing; Performance indicators; Thermal vapour compression

1. Introduction

Insufficient access to drinking water is one of the most widespread problems in the world. In fact, the fresh water resources represent only 2.5% of the volume of water existing on Earth [1], but its use in the industrial, agricultural and household sectors is becoming increasingly important. Today, 40% of the world population lives within 100 km of the sea, which means that potentially 2.4 billion people can be supplied with drinking water through desalination technology [1]. Therefore, large number of desalination plants is currently in operation in several countries. Indeed, according to the International Desalination Association, in June 2015, more than 18,000 desalination plants operated worldwide, producing about 87 million m^3 d^{-1}, providing water for 300 million people [2].

There are several technologies for desalination of sea and brackish water, but multistage flash desalination process (MSF-BR and MSF-OT) is the largest sector in the seawater desalination industry. It accounts for more than 40% of the entire desalination market [2]. Unfortunately, this process is energy intensive in comparison with other desalination processes. Indeed, the energy consumption of desalination processes is 18 kWh m^{-3} for MSF, 15 kWh m^{-3}

* Corresponding author.

for multiple effect evaporation, and 5 kWh m^{-3} for reverse osmosis (RO) [3]. Then it is therefore, essential to search novel MSF designs, which lead to reduction of energy consumption and consequently lower water production cost.

Literature review of studies on the MSF system shows the existence of several studies aimed at improving the overall performance of the MSF process [4–14], among which the development of novel MSF configurations. The study presented by Helal et al. [12] explored the feasibility of the hybridization of RO and MSF process. The results obtained show that the water cost of the MSF process can be reduced by 17% to 24% through hybridization with RO technology. This improvement would be greater if the hybrid MSF-RO installation is coupled to nuclear reactor, as reported by Al-Mutaz [8].

The study presented by Mabrouk et al. [11] focused on analysis of coupling a mechanical vapour compression distiller with a multi-stage-flash evaporator (MSF-MVC). The obtained results show that the performance ratio of the proposed MSF–MVC system was 2.4 times the performance ratio of the conventional MSF process, and the unit product cost is 25% less than that of the conventional MSF process.

Nafey et al. [14] studied a hybrid multi-effect evaporation-multi stage flash (MEE-MSF) system. The obtained results show that this configuration is more economical than either standalone MSF or MEE system. Indeed, comparison between MSF (20 stages), MEE (10 effects), and the hybrid MEE-MSF (10 modules) showed that the unit product cost of the hybrid MEE-MSF system is obtained as 1.7 \$ m^{-3}, which is 31% less than that of the MSF (2.63 \$ m^{-3}) system and 9% less than that of the MEE (1.87 \$ m^{-3}).

El-Dessouky et al. [15] proposed a combination of thermal vapour compression (TVC) with the multistage flash desalination process with brine recirculation MSF-BR. Results obtained show a significant improvement in the performance indicators in comparison with the conventional configuration. Indeed, for a 24-stage MSF-BR/TCV installation operating at a top brine temperature of 110°C. The thermal performance ratio increases by 14%, and the speciifc flow rate of cooling water decreases by 8%.

The advantages obtained when coupling TVC with MSF-BR, motivated us to study in this work the effects on performance indicators when we combine the once-through multistage flash desalination with TVC, MSF-OT/TCV.

The following sections include a brief description of the MSF-OT/TVC process, a detailed mathematical model of the MSF-OT/TCV process, the results and discussion as well as some concluding remarks.

2. Description of the MSF-OT/TCV desalination process

The schematic diagram of the MSF-OT/TVC system is given in Fig. 1. As is shown, the system comprises essentially a steam jet ejector, a brine heater and a series of flashing stages. Fig. 2 shows a schematic representation of the flashing stage. It includes a brine pool, vapour space, demister, condenser tubes, distillate-collecting tray, and inlet/outlet brine orifices.

The feed seawater (M_f) is filtered, deaerated, chemically treated, and then passes in the condenser tubes across the stages; its temperature increases from T_f to t_1 before entering

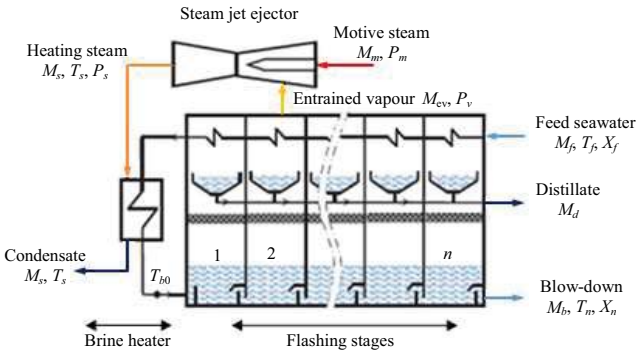

Fig. 1. Scheme of once-through multistage flash desalination process combined with thermal vapour compression, MSF-OT/TVC (a)

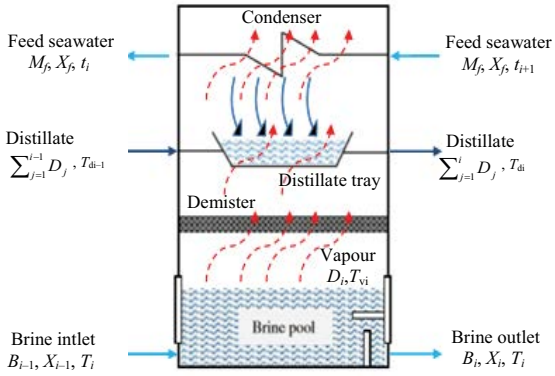

Fig. 2. Scheme of the *i*-th stage of a MSF-OT/TVC plant.

the brine heater, which has a shell and tube configuration. The heating steam flows on the shell side, and the feed seawater through the tube side. Frequently, the heating steam enters the heater through several orifices along the length of the heater in order to obtain a uniform distribution of the temperature within the heater. Passing through the brine heater, the brine stream absorbs the latent heat of the heating steam (M_s), thus its temperature increases to its maximum value (T_{b0}) called top brine temperature. This value depends on the nature of chemicals used to control the scale formation. The heated brine then enters the first flashing stage through a submerged orifice that reduces the pressure and increases turbulence. As the brine was already in the saturated liquid state at the exit of the brine heater, it will become superheated and flashes to give off a small amount of water vapour. As is shown in Fig. 2, this vapour passes through a wire demister to remove entrained brine droplets, and on tubes condenser (preheater), where it releases its latent heat and condenses. This heat recovery improves the process efficiency because of reducing the heating energy consumption. The condensed vapour accumulates in the distillate tray located below the condenser. This process is then repeated all the way down the plant as both brine and distillate enter the next flashing stage, which is at a lower pressure. Finally, in the last stage of the plant, the brine blow-down (M_b) is rejected to the sea and the distillate product stream (M_d) is collected.

The steam jet ejector supplies the brine heater with heating steam (Fig. 1). Indeed, a high-pressure motive steam drawn from a boiler, compresses a specified portion of the vapour formed in the flashing stages to a temperature T_s depending on the desired maximum heating temperature of the brine T_{b0}. The compressed vapour is then used to heat brine stream in the brine heater. The use of ejectors as heat pump is motivated by their many advantages compared with mechanical compression. Indeed, their construction is simple and rugged, they have the capability of handling enormous quantity of steams with relatively small sizes of equipment, they are very reliable since they need less maintenance requirements, and finally they are of simple operation because of the absence of moving parts.

The role of the steam jet ejectors is to transport and compress a flow of induced fluid from the suction pressure to the desired exit pressure. Fig. 3 shows a description of the steam jet ejector. It consists of converging-diverging nozzle, mixing chamber, and a converging-diverging diffuser. The motive steam (M_m), having a high pressure, enters in the nozzle where its static pressure energy is converted to kinetic energy. At the nozzle outlet, the motive steam velocity became supersonic, it induces a region of low-pressure flow, which causes the steam extracted from flashing stages (M_{ev}) to become entrained and mixed with the actuating steam in the mixing chamber. The two fluids (M_m and M_{ev}) are then recompressed through the diffuser by rapid deceleration: First, they continue to mix, while they move through the converging section of the diffuser, and at the entrance to the throat, they become completely mixed. Then, passing in the diverging section, the pressure of the mixture increases and speed decreases. At the end, the mixed stream is charged at an intermediate pressure (P_s), which is higher than the entrained steam pressure (P_v), but much lower than the inlet motive steam pressure (P_m). The stream will then be directed to the brine heater [16]. The steam jet ejector is designed to operate at the critical condition, where the pressure compression ratio (P_s/P_v) is greater than 1,81 [15].

In this study, three configurations that differ in the location of vapour entrainment are considered. In the first, vapour is entrained from the second stage, corresponding to the high temperature stage, in the second, vapour is entrained from the stage 10, corresponding to the middle temperature stage, and in the third, vapour is entrained from the last stage, corresponding to the low temperature stage. In the all configurations, vapour is compressed to a temperature given a top brine temperature T_{b0} ranging from 90°C to 110°C.

3. Mathematical model of MSF-OT/TCV

The steady-state mathematical model of the MSF-OT/TCV process is constituted of set of mass and energy balance equations for the flashing stages, brine heater, and steam ejector. The model has been developed using the following assumptions:

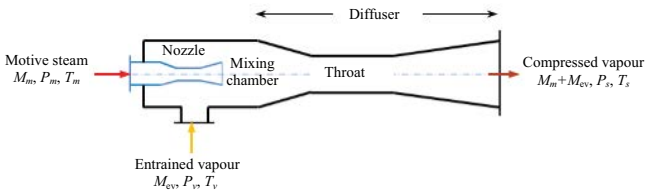

Fig. 3. Schematic description of the steam jet ejector.

- Stage condensers have equal heat transfer area, A_c.
- Thermo-physical properties for feed seawater, and brine depend on temperature and salt concentration.
- Thermo-physical properties for distillate product, heating steam, and vapour produced in stages are functions of temperature.
- The overall heat transfer coefficients U_c, in the condensers depend on the following parameters:
  - Flow rate of the condensing vapour.
  - Flow rate of the feed seawater flowing inside the condenser tubes.
  - Temperatures of the condensing vapour and feed seawater flowing inside the condenser tubes.
  - Physical properties of the condensing vapour and feed seawater flowing inside the condenser tubes.
  - The tube material, diameter, and wall thickness.
  - The fouling resistance.
  - Thermodynamic losses include the boiling point elevation (BPE) and the non-equil.ibrium allowance (NEA).

Other simplifying assumptions, having negligible effect on the accuracy of model predictions, are adopted in model development. These assumptions are as follows:

- Distillate product is salt free.
- Condensate produced in the brine heater is not sub cooled.
- Heat losses to the surroundings are negligible.
- Effect of no condensable gases on heat transfer is negligible.
- Electrical energy used by pumps is not considered in the system analysis.

The parameters and variables used for the development of model equations are shown in Figs. 1–3. El-Dessoukey and Ettouney [17] give the expressions of the thermo-physical characteristics of the different streams of the process.

The brine mass balance in stage (i) is given by:

$$B_{i-1} = B_i + D_i \tag{1}$$

For the first stage, the term B_{i-1} is equal to M_f. Consequently, the mass balance for this stage becomes as follows:

$$M_f = B_1 + D_1 \tag{2}$$

The stage salt balance is given by:

$$X_{i-1}B_{i-1} = X_iB_i \tag{3}$$

For the first stage, B_{i-1} is equal to M_f and X_{i-1} equal to X_f. Consequently, the salt balance in the first stage is given by:

$$X_fM_f = X_1B_1 \tag{4}$$

The energy balance for the flashing brine is given by:

$$D_i\lambda_{vi} = B_{i-1}C_{pbi-1}\left(T_{i-1} - T_i\right) \tag{5}$$

λ_{vi}, is the latent heat of flashing vapour, calculated at the vapour temperature T_{vi} is given by:

$$T_{\mathrm{vi}} = T_i - \mathrm{NEA}_i - \mathrm{BPE}_i \tag{6}$$

The BPE is the increase in the brine boiling temperature due to the effect of dissolved salts. It depends on the brine temperature and salt concentration. The NEA is the quantification of the irreversible phenomena that characterize the flashing process in the boiling pool [18]. NEA depends on the stage flashing range, $T_{i-1} - T_i$, the vapour temperature, T_{vi}, the flow rate of the brine B_i, and the stage geometry.

For the first stage, B_{i-1} is equal to M_f and T_{i-1} is equal to the top brine temperature T_{b0}. Consequently, the brine energy balance in the first stage is given by:

$$D_1\lambda_{v1} = M_f C_{\mathrm{pb}}\left(T_{b0} - T_1\right) \tag{7}$$

The energy balance for the condenser tubes is given by:

$$D_i\lambda_{\mathrm{ci}} + C_{\mathrm{pdi}}\left(T_{\mathrm{di-1}} - T_{\mathrm{di}}\right)\sum_{k=1}^{i-1} D_k = M_f C_{\mathrm{pfi}}\left(t_i - t_{i+1}\right) \tag{8}$$

In the first stage, the term $\sum_{k=1}^{i-1} D_k$ is equal to zero. Consequently, the condenser energy balance in the first stage is given by:

$$D_1\lambda_{c1} = M_f C_{\mathrm{pf1}}\left(t_1 - t_2\right) \tag{9}$$

In the last stage, the temperature t_{i+1} is equal to t_f. Consequently, the condenser energy balance in the last stage is given by:

$$D_n\lambda_{\mathrm{cn}} + C_{\mathrm{pdn}}\left(T_{\mathrm{dn-1}} - T_{\mathrm{dn}}\right)\sum_{k=1}^{n-1} D_k = M_f C_{\mathrm{pfn}}\left(t_n - t_f\right) \tag{10}$$

In the stage where the entrained vapour M_{ev} is extracted by the steam jet ejector, the condenser energy balance is given by:

$$\left(D_i - M_{\mathrm{ev}}\right)\lambda_{\mathrm{ci}} + C_{\mathrm{pdi}}\left(T_{\mathrm{di-1}} - T_{\mathrm{di}}\right)\sum_{k=1}^{i-1} D_k = M_f C_{\mathrm{pfi}}\left(t_i - t_{i+1}\right) \tag{11}$$

The heat transfer equation for the condenser tubes, having a heat transfer surface A_c, is given by:

$$M_f C_{\mathrm{pfi}}\left(t_i - t_{i+1}\right) = U_i A_c \left(\mathrm{LMTD}\right)_i \tag{12}$$

The expression of $(\mathrm{LMTD})_i$ is given by:

$$\left(\mathrm{LMTD}\right)_i = \frac{\left(t_i - t_{i+1}\right)}{\ln\left[\left(T_{\mathrm{ci}} - t_{i+1}\right)/\left(T_{\mathrm{ci}} - t_{\mathrm{i}}\right)\right]} \tag{13}$$

The heat transfer equation for the brine heater, having a heat transfer surface A_h, is given by:

$$M_f C_{\mathrm{ph}}\left(T_{b0} - t_1\right) = U_h A_h \left(\mathrm{LMTD}\right)_h \tag{14}$$

The expression of $(\mathrm{LMTD})_h$ is given by:

$$\left(\mathrm{LMTD}\right)_h = \frac{\left(T_{b0} - t_1\right)}{\ln\left[\left(T_s - t_1\right)/\left(T_s - T_{b0}\right)\right]} \tag{15}$$

The heat steam temperature, T_s, is taken higher than the top brine temperature, T_{b0}, by 10°C:

$$T_s = T_{b0} + 10 \tag{16}$$

The equation giving the total flow rate of the product distillate, M_d, is given by:

$$M_d = M_{\mathrm{ev}} + \sum_{i=1}^{n} D_i \tag{17}$$

The equation giving the steam flow rate M_s is given by:

$$M_s = M_m + M_{\mathrm{ev}} \tag{18}$$

The modelling of the steam jet ejector adopted in this work was previously developed by El-Dessouky et al. [15]. It includes two equations. The first one concerns the compression ratio, C_r, which is given by:

$$C_r = \frac{P_s}{P_v} \tag{19}$$

The compression ratio can be varied over a range from 1.8 to 5. The second equation concerns the entrainment ratio, Ra. It is defined as the mass flow rate of motive steam to the mass flow rate of entrained vapour, and it is expressed by:

$$\mathrm{Ra} = \frac{M_m}{M_{\mathrm{ev}}} = 0.296\frac{\left(P_s\right)^{1.19}}{\left(P_v\right)^{1.04}}\left(\frac{P_m}{P_v}\right)^{0.015}\left(\frac{\mathrm{PCF}}{\mathrm{TCF}}\right) \tag{20}$$

PCF is the motive steam pressure correction factor and TCF is the entrained vapour temperature correction factor. They are given by:

$$\mathrm{PCF} = 3\times10^{-7}\left(P_m\right)^2 - 9\times10^{-4}P_m + 1.6101 \tag{21}$$

$$\mathrm{TCF} = 2\times10^{-8}\left(T_v\right)^2 - 6\times10^{-4}T_v + 1.0047 \tag{22}$$

The steam at the exit ejector and the entrained vapour are in the saturated vapour state. Therefore the expressions of P_v and P_s are given by:

$$P_v = 10.17246 - 0.6167302T_v + 1.832249\times10^{-2}T_v^2 - 1.77376\times10^{-4}T_v^3 + 1.47068\times10^{-6}T_v^4 \tag{23}$$

$$P_s = 10.17246 - 0.6167302T_s + 1.832249\times10^{-2}T_s^2 - 1.77376\times10^{-4}T_s^3 + 1.47068\times10^{-6}T_s^4 \tag{24}$$

The pressures (P_m, P_v, P_s), temperatures (T_v, T_s), and flow rates (M_m, M_{ev}) in the above equations are in kPa, °C, and kg s^{-1}, respectively. The above equations are valid in the following ranges: Ra ≤ 5.5, 10 < T_v ≤ 500°C, 100 ≤ P_m ≤ 3,500 kPa, and 1.81 ≤ C_r.

4. Solution procedure

The mathematical modelling of the MSF-OT/TCV process, presented in the previous section, gave us a system of algebraic and highly nonlinear equations. In fact, the dependence of the thermophysical properties of different fluids flowing in the installation on the temperature and salt concentration are the main contributors to the complexity and non-linearity of the equations.

The unknowns of the system of equations are the distillate flow rate produced in each stage (D_1,…,D_n), the outlet brine mass flow rate (B_1,…,B_n), the outlet brine salinity (X_1,…,X_n), the stage temperature (T_1,…,T_n), the seawater temperature at the outlet of the condenser tubes (t_1,…,t_n), the total production capacity (M_d), the make-up mass flow rate (M_f), the top brine temperature (T_{b0}), the motive steam flow rate (M_m), the entrained vapour flow rate (M_{ev}), the steam flow rate (M_s), and the steam temperature (T_s). The total number of unknowns is ($5n + 7$), however, there are ($5n + 5$) independent system equations. Therefore, two unknowns of the system must be specified to be able to solve the system. In this work, we consider performance calculation for the MSF-OT/TCV process. Thus, the parameters whose values were specified are: the distillate production (M_d), and the top brine temperature (T_{b0}), as it is recommended by Helel et al. [19].

The system was solved through an iterative procedure. In each itération we used the solver fsolve of MATLAB software. This solver uses the trust-region-reflective algorithm for solving systems of nonlinear equations. The initial values of the unknowns of the system (first iteration) were obtained by previously solving equations obtained using a simplified modelling of the process [17]. This simplified model is based on the following assumptions:

- Specific heat at constant pressure, Cp, for all liquid streams, brine, distillate, and seawater is constant and equal to 4.18 kJ kg^{-1} °C.
- Temperature drop per stage for the flashing brine is constant and equal to ($T_{b0} - 40$)/n.
- Temperature elevation per stage for the feed brine is constant and equal to [($T_{b0} - 5$) – t_f]/n.
- Latent heat of vapourization and condensation (λ_v, λ_c) is constant and equal to 2,412 kJ kg^{-1}.
- Thermodynamic losses in all the stages are constant and equal to 2°C.
- The overall heat transfer coefficient in the brine heater (U_h) and condensers (U_c) is constant and equal to 2 kW m^{-2} °C.

Fig. 4 shows a schema describing the method of solving the system of equations.

5. Results and discussion

Table 1 gives the installation's characteristics used for this study. They are those reported by Ben Ali et al. [20]

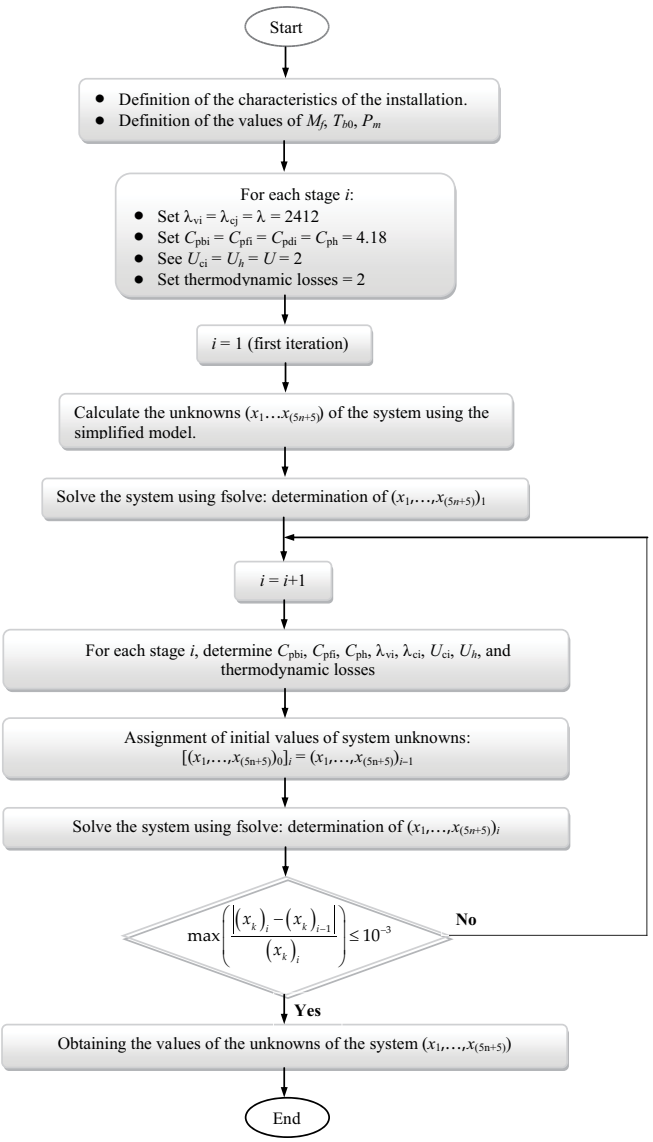

Fig. 4. Flowchart of the method of solving the system of equations.

during a previous study of an MSF-OT installation, with the exception of the steam ejector whose characteristics are given by El-Dessouky et al. [15].

Three configurations are considered in this study that differs in the location of vapour entrainment and number of ejectors used. In the first configuration (Fig. 1), we used only one ejector, and vapour is entrained from the second stage. As is shown in Fig. 5, in the second configuration, vapour is entrained from a middle position of installation (stage 10). The low value of the temperature of the vapour produced in this stage forced us to use two ejectors in series, also because vapour compression gives compression ratio of 5.71 which is upper than the maximum limit. In the third configuration (Fig. 6), vapour is entrained from the last stage. For the same reason, we used two ejectors in series because vapour compression gives a compression ratio of 8.23.

Table 1
Values of the parameters used for the studied MSF-OT/TVC installation

Parameter	Value
Number of stages (n)	21
Stage width	17.660 m
Stage length	3.150 m
Stage height	4.521 m
Number of condenser tubes	1,410
Heat transfer area of condenser, A_c	3,380 m^2
Condenser tubes outer diameter	0.0445 m
Condenser tubes inner diameter	0.04197 m
Material of the condenser tubes	Cu/Ni 90/10
Density of the demister	80.317 kg m^{-3}
Thickness of the demister	0.200 m
Area of the demister	19.426 m^2
Number of brine heater tubes	3,800
Heat transfer area of brine heater, A_h	3,530 m^2
Brine heater tubes outer diameter	0.0244 m
Brine heater tubes inner diameter	0.0220 m
Material of brine heater tubes	Titanium
Range for the top brine temperature, T_{b0}	90°C–110°C
Temperature of reject brine, T_n	40°C
Intake sea water temperature, T_f	30°C
Salinity of intake seawater, X_f	40,000 ppm
Motive steam pressure, P_m	1,500 kPa
Compression ratio for the steam jet ejector, C_r	<5

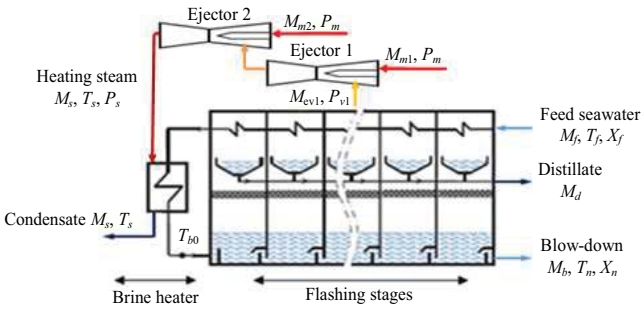

Fig. 5. MSF-OT/TVC (b), Vapour entrainment from the middle stage.

In the first part, we looked at comparing the performance indicators of the three configurations studied with the conventional configuration (MSF-OT). These indicators are as follows:

- The thermal performance ratio which is the ratio of distillate flow rate to the motive steam flow rate, PR = M_d/M_m
- The specific flow rate of feed seawater, $sM_f = M_f/M_d$.

Fig. 7 gives variations in the thermal performance ratio for the three MSF-OT/TVC configurations and for the conventional MSF-OT configuration. The thermal performance ratio grows up when the top brine temperature is increased. This is explained by the use of less amount of heating steam (motive steam in the MSF-OT/TCV configuration) to produce constant distillate rate. The highest thermal performance ratio is obtained when the entrained vapour is extracted from the hot side of the installation (configuration a). Its value varies from 12.27 to 19.20 when the top brine temperature varies from 90°C to 110°C. On average, the thermal performance ratio of the first MSF-OT/TVC configuration is 49.22% greater than that of the conventional MSF-OT configuration. Thus, the first MSF-OT/TCV configuration has the best thermal energy efficiency in comparison with other configurations.

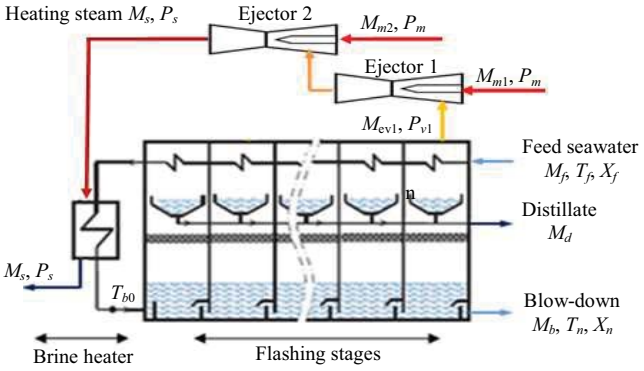

Fig. 6. MSF-OT/TVC (c), Vapour entrainment from the last stage.

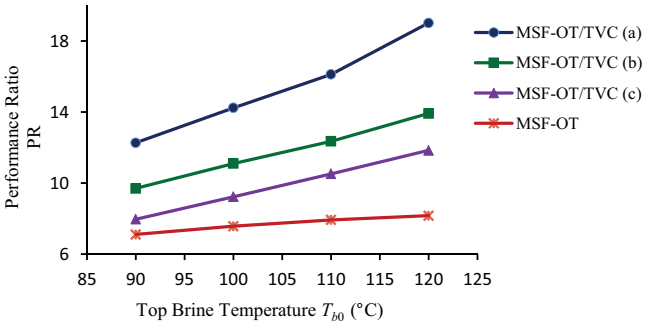

Fig. 7. Variation in thermal performance ratio as a function of the top brine temperature.

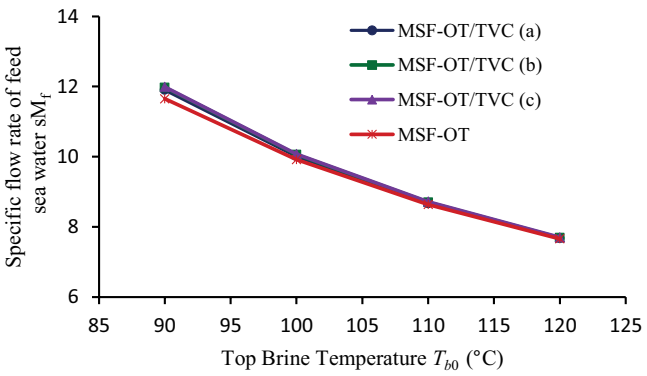

Fig. 8. Variation in specific flow rate of feed seawater as a function of the top brine temperature.

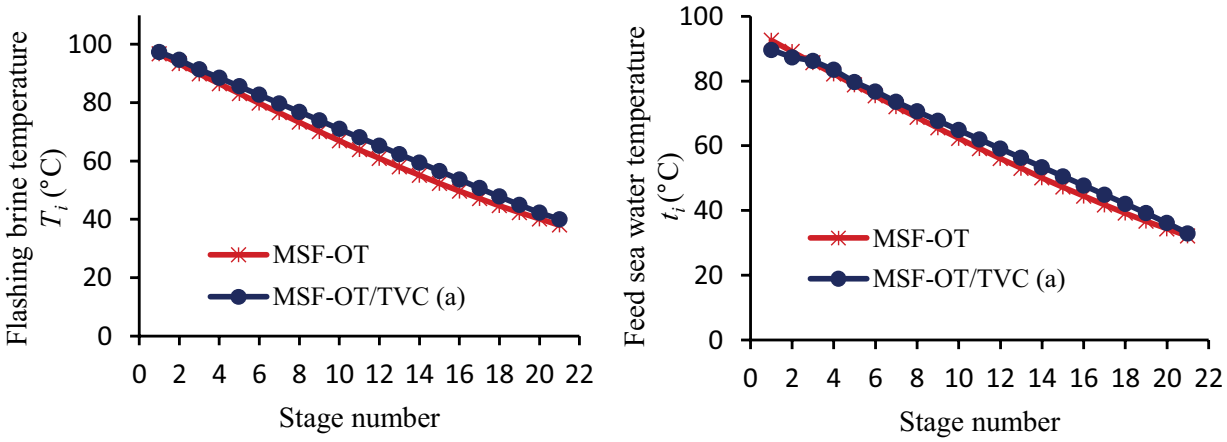

Fig. 9. Temperature profiles for the flashing brine, and for seawater flowing in the condenser tubes.

Variations in the specific flow rate of feed seawater are shown in Fig. 8 for the three MSF-OT/TCV configurations and for the conventional MSF-OT configuration. As is shown, the specific flow rate of feed seawater decreases with the increase in the top brine temperature. We note that the use of the thermal compression vapour has no influence on specific flow rate of feed seawater. The difference between the first MSF-OT/TCV configuration and that of the conventional MSF-OT configuration does not exceed 1%. For the MSF-OT/TCV configurations, its value varies from 11.9 to 7.6 when the top brine temperature varies from 90°C to 110°C.

The results obtained above concerning the performance indicators show a significant gain obtained when the MSF-OT/TCV process with extraction of the entrained vapour from the hot side of the installation (first configuration) is used. Therefore, in the following, we show the temperature profiles, brine flow rate, and brine salinity, only for the first MSF-OT/TCV configuration and the conventional MSF-OT configuration.

Fig. 9 shows the temperature profiles for the flashing brine (T_i), and seawater flowing in the condenser tubes (t_i). We find that they are identical for both configurations. This is because the temperature drop per stage of the flashing brine and the temperature difference of the feed seawater flowing inside condensers are similar for the two configurations. The same behavior was observed for the profiles of brine flow rate, and brine salinity depicted in Figs. 10 and 11, respectively. Indeed, since distillate is salt free, the results show that the brine salinity increases as the flashing brine flow rate decreases in each stage.

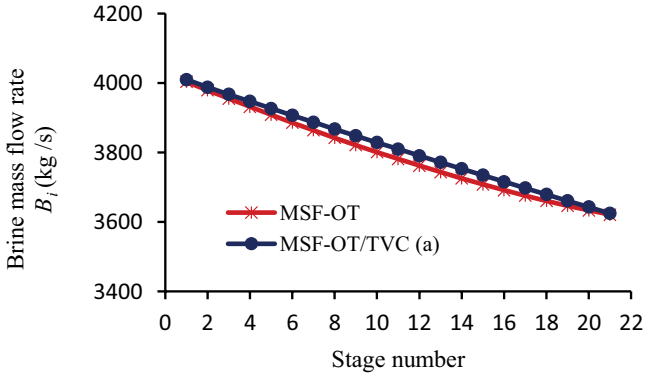

Fig. 10. Brine flow rate at each stage.

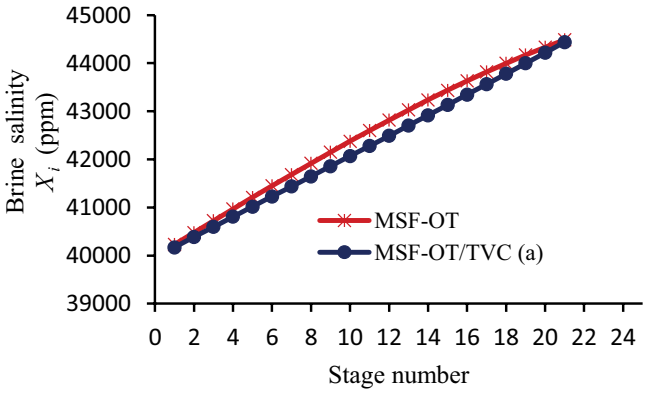

Fig. 11. Brine salinity at each stage.

6. Conclusion

In this study, we investigate a novel configuration of the MSF-OT system, where the TVC is used to produce heating steam used by the heat input section. In the first part of the study an algorithm is presented and it is used for solving the large system of algebraic and non-linear equations describing the steady-state model of three MSF-OT/TCV configurations. The systems of equations were solved through an iterative procedure by using a solver of MATLAB toolboxes. Analysis of the results shows:

- Thermal vapour compression improves significantly thermal performance ratio, but it increases slightly the specific feed seawater flow rate.
- Using a entrained vapour from stages in the hot side of the installation gives the highest thermal performance ratio.
- The effect of vapour compression is negligible on the temperature, flowrate and salinity profile of the flashing brine.

- The top brine temperature, T_{b0}, plays an important role on the performance of the MSF-OT/TCV system. By increasing the T_{b0}, the thermal performance ratio increases and the specific feed seawater decreases.

Symbols

A	—	Heat transfer area, m^2
B	—	Flashing brine mass flow rate, kg s^{-1}
BPE	—	Boiling point elevation, °C
Cp	—	Specific heat at constant pressure, kJ kg^{-1} K^{-1}
C_r	—	Compression ratio
D	—	Distillate formed in each flashing stage, kg s^{-1}
LMTD	—	Logarithmic mean temperature difference, °C
M	—	Mass flow rate, kg s^{-1}
n	—	Total number of stages
NEA	—	Non-equilibrium allowance, °C
PR	—	Thermal performance ratio
P	—	Pressure, kPa
Ra	—	Entrainment ratio
sM_f	—	Specific feed seawater flow rate
T	—	Brine temperature, °C
TVC	—	Thermal vapour compression
t	—	Temperature of seawater flowing in condenser tubes, °C
T_{b0}	—	Top brine temperature, °C
U	—	Overall heat transfer coefficient, W m^{-2} K^{-1}
X	—	Water salinity, ppm

Greek

λ	—	Latent heat of vaporization, kJ kg^{-1}

Subscripts

b	—	Brine
c	—	Condenser or condensate
d	—	Distillate product
ev	—	Entrained vapour
f	—	Feed
h	—	Brine heater
m	—	Motive steam
s	—	Steam
v	—	Vapour

References

[1] Bennet, M. Cuccinello, Saltwater Desalination in Water Treatment Primer, Seawater Desalination in Mediterranean Countries, Venice, Italy, 28–31 May, 2001.

[2] *Henthorne, Lisa,* The Current State of Desalination, International Desalination Association, September 5, 2016.

[3] M. Al-Sahali, H. Ettouney, Developments in thermal desalination processes: design, energy, and costing aspects, Desalination, 214 (2007) 227–240.

[4] K.A. Al-Shayji, S. Al-Wadyei, A. Elkamel, Modelling and optimization of a multistage flash desalination process, Eng. Optim., 37 (2005) 591–607.

[5] M.S. Tanvir, I.M. Mujtaba, Optimization of design and operation of MSF desalination process using MINLP technique in gPROMS, Desalination, 222 (2008) 419–430.

[6] A.M. E1-Nashar, Optimization of operating parameters of MSF plants through automatic setpoint control, Desalination, 116 (1998) 89–107.

[7] M.H.K. Manesh, M. Amidpour, Multi-objective thermoeconomic optimization of coupling MSF desalination with PWR nuclear power plant through evolutionary algorithms, Desalination, 249 (2009) 1332–1344.

[8] I.S. Al-Mutaz, Coupling of a nuclear reactor to hybrid RO-MSF desalination plants, Desalination, 157 (2003) 259–268.

[9] G. Calì, E. Fois, A. Lallai, G. Mura, Optimal design of a hybrid RO/MSF desalination system in a non-OPEC country, Desalination, 228 (2008) 114–127.

[10] A.D. Khawaji, I.K. Kutubkhanah, J.-M. Wie, Advances in seawater desalination technologies, Desalination, 221 (2008) 47–69.

[11] A.A. Mabrouk, A.S. Nafey, H.E.S. Fath, Analysis of a new design of a multi-stage flash–mechanical vapour compression desalination process, Desalination, 204 (2007) 482–500.

[12] A.M. Helal, A.M. El-Nashar, E.S. Al-Katheeri, S.A. Al-Malek, Optimal design of hybrid RO/MSF desalination plants: Part II: results and discussion, Desalination, 160 (2004) 13–27.

[13] Y.M. El-Sayed, Designing desalination systems for higher productivity, Desalination, 134 (2001) 129–158.

[14] A.S. Nafey, H.E.S. Fath, A.A. Mabrouk, Thermo-economic investigation of multi effect evaporation (MEE) and hybrid multi effect evaporation—multi stage flash (MEE-MSF) systems, Desalination, 201 (2006) 241–254.

[15] H. El-Dessouky, H. Ettouney, H. Al-Fulaij, F. Mandani, Multistage flash desalination combined with thermal vapour compression, Chem. Eng. Process., 39 (2000) 343–356.

[16] B.R. Power, Steam Jet Ejectors for Process Industries, McGraw Hill, New York, 1994.

[17] H.T. El-Dessouky, H.M. Ettouney, Fundamentals of Salt Water Desalination, Elsevier Science, Amsterdam, 2002.

[18] P. Fiorini, E. Sciubba, C. Sommariva, A new formulation for the non-equilibrium allowance in MSF processes, Desalination, 136 (2001) 177–188.

[19] A.M. Helal, M.S. Medani, M.A. Soliman, J.R. Flower, A tridiagonal matrix model for multistage flash desalination plants, Comput. Chem. Eng., 10 (1986) 327–341.

[20] M. Ben Ali, L. Kairouani, Solving equations describing the steady-state model of MSF desalination process using Solver Optimization Tool of MATLAB software, Desal. Wat. Treat., 52 (2014) 7473–7483.